MICROSTRUCTRAL MODELING OF THE FRACTURE TOUGHNESS OF 7000 AL ALLOYS

Ph. Achon*,1, J.C. Ehrström** and A. Pineau*

Fracture toughness tests have been carried out on two Al alloys (7075 and 7475) with different amounts of Fe and Si. These materials were tested under T3, T6 and T7 conditions along 6 directions (LT, LS, TL, TS, SL and ST). Quantitative metallography was largely applied to measure the volume fraction of intermetallic particles (Mg_2Si and Fe rich precipitates), the mean size of these particles and their distribution on different section planes. Three micromechanical models were used to explain the large variations observed for the fracture toughness (20-60 MPa$\sqrt{m}$). It is shown that these variations can be explained by taking into account the non-homogeneous distribution of intermetallic phases.

INTRODUCTION

It is well known that the fracture toughness of high strength Al alloys is strongly dependent on their composition, in particular their content in residual elements such as Fe and Si, and on the fabrication parameters. It is also well established that the fracture toughness of Al alloys plates is strongly anisotropic. However there are relatively few quantitative studies devoted to the modeling of the fracture toughness of these materials in relation with their microstructure, in particular the distribution of Fe rich and Mg_2Si particles responsible for the nucleation of cavities. The main aim of the present study was to correlate the values of the fracture toughness determined in various directions of thick plates with the distribution of these particles. This correlation was based on three models which were proposed previously for ductile fracture.

* Centre des Matériaux, Ecole des Mines, BP.87, 91003 Evry (France), URA CNRS 866.
** Centre de Recherches Péchiney, BP.27, 38340 Voreppe (France).
1 Now with Institut de Soudure, Centre A. Leroy, 57365 Ennery (France)

MATERIALS AND EXPERIMENTAL PROCEDURES

The materials investigated were hot rolled commercial Al-6 Zn-2.50 Mg-1.50 Cu alloy plates of 50 mm thickness. Their composition is given in Table 1. Alloy 7075 contained a much higher content in Si and Fe as Alloy 7475. These elements are responsible for the formation of relatively large intermetallic phases of type Mg_2Si and Al_7Cu_2Fe + $Al_{23}CuFe_4$, respectively. Both materials were investigated in three conditions : (i) Aged at room temperature (T351), (ii) Peakaged : 120°C - 24 hours (T651), and (iii) Overaged : 105°C - 6 hours + 160°C - 24 hours (T7351). The grain microstructure of both alloys was unrecrystallized with a pancake shape (1x0.4x0.05 mm^3). They were strongly textured with two components : {110} <112> brass and S {123} <634>.

TABLE 1 - Chemical compositions (Wt pct)

Alloy	Si	Fe	Mn	Ti	Cr	Cu	Mg	Zn
7075	0.070	0.180	0.047	0.020	0.24	1.48	2.64	5.71
7475	0.039	0.050	0.022	0.017	0.21	1.52	2.33	5.85

Fracture toughness tests were carried out along 6 orientations : LT, LS, TL, TS, SL and ST. CT 30 mm specimens were used for the LT, LS, TL and TS orientations while CT 20 mm were used for the two other orientations. In the T6 condition the test results could be interpreted in terms of valid K_{IC} while in the two other conditions J_{IC} was measured according to the ASTM E813 standards. These values of J_{IC} were converted into K_{JC} by $K_{JC} = [E\, J_{IC}/(1-\nu^2)]^{1/2}$.

Quantitative metallography was largely used to measure the distribution in Mg and Fe rich particles. The number of inclusions Nai (i = L, T, S) per unit area and their size were measured on three section planes. The total number of particles per unit volume, Nv was determined. The results of these measurements are given in Table 2 where it is observed that the volume fraction of intermetallic phases is about 4 times larger in 7075 alloy than in 7475 alloy. The mean particle size in both materials was found to be : (i) 7075 alloy : Mg_2Si (14.4 x 7.7 x 3.5 μm^3), Fe rich (6.7 x 4.8 x 2.5 μm^3); (ii) 7475 : Mg_2Si (5.8 x 8.4 x 3.8 μm^3), Fe rich (5.4 x 5 x 2.3 μm^3). These particles were grouped into clusters aligned along the rolling direction. These clusters were also quantitatively analyzed. Full details can be found elsewhere [1].

TABLE 2 - Volume fraction of intermetallic particles

Alloy	fv(%)		$\Sigma \bar{f}_V$(%)	N_V (10^3 mm^3)		$\Sigma \bar{N}_V$ (10^3 mm^3)
	Mg_2Si	Fe		Mg_2Si	Fe	
7075	0.166	1.024	1.190	11	148.3	159.3
7475	0.066	0.277	0.343	3.9	71.1	75

RESULTS AND DISCUSSION

The results of tensile tests performed on 7475 alloy are reported in Table 3. Alloy 7075 had similar mechanical properties. The work hardening exponent, n, was found to be : n = 0.17 in the T3 condition, n = 0.10 in T6 and n = 0.11 in T7 conditions.

The results of fracture toughness tests are shown in Fig.1 where it is observed that alloy 7475 is much tougher than alloy 7075, as expected. Moreover it is observed that K_{IC} T3 > K_{IC} T7 > K_{IC} T6. It is also noticed that the orientation has a strong influence on the fracture toughness : K_{IC} L - (TS)) > K_{IC} T - (LS) > K_{IC} S - (LT).

TABLE 3 - Mechanical properties of 7475 alloy

	L			T			S		
	T3	T6	T7	T3	T6	T7	T3	T6	T7
Rp0.2 (MPa)	447	523	452	414	506	449	343	447	416
U.T.S. (MPa)	578	588	519	565	578	514	523	545	504

In the first model used to interpret these results it was assumed that the calculated crack tip opening displacement, CTOD was equal to the mean distance between intermetallic particles in a plane perpendicular to the crack front, λ, where $\lambda = 1/2 \sqrt{Nai}$, (i = L,T,S). The value of J_{IC} was related to that of the CTOD by the expression derived by McMeeking [2], i.e :

$$J_{IC} = M \cdot Rp_{0.2} \cdot (CTOD) \qquad (1a)$$

where $$1/M = 0.54\,(1+n)[2/\sqrt{3}\,.\,(1+v)\,.\,(1+n)\,/\,n\,.\,Rp_{0.2}\,/\,E]^n \qquad (1b)$$

The results obtained with this first model are compared to the experimental data in Fig.2. In this figure, as in the following , we have drawn lines corresponding to a certain difference (± 10%, ± 20%, ± 50%) between the calculated values and the observed ones. This simple model which requires only the knowledge of the number of particles in three planes and the mechanical properties ($Rp_{0.2}$, n) of the materials in three directions is able to account qualitatively for the difference in the behaviour of both alloys. However it is systematically observed that this model overpredicts the values of the fracture toughness, in particular in the T6 and T7 conditions.

The second model was previously used to predict the variation of the fracture toughness of low alloy steels in which ductile fracture initiates also from inclusions, [3]. In this model it is assumed that fracture takes place when the mean cavity growth rate, $\langle R/R_0 \rangle$, calculated ahead of the crack tip is equal to the cavity growth rate, (R/R_0) measured on notched specimens. The results of these measurements are given in Table 4. $\langle R/R_0 \rangle$ is expressed as :

$$\langle R / R_0 \rangle_\delta = \frac{1}{B} \int_{-B/2}^{+B/2} \int_{-\theta}^{+\theta} \int_0^{\infty} [R(x,\theta) / R_0] \; f(x,\theta,z) dx \; d\theta \; dz \quad (2)$$

where B is the thickness of the specimens, $-\pi/4 \leq \theta \leq \pi/4$, R_0 is the mean size of the intermetallic particles, R (x, θ)/R_0 is obtained from F.E. calculations, while f (x,θ,z) represents the probability of finding one inclusion at a position (x,θ,z) from the crack tip. Full details are given elsewhere [1]. It was assumed that the particles were distributed according to a Poisson law. The results obtained from this model are shown in Fig.3 where it is observed that this approach gives more satisfactory results than the first one, in particular for the T6 and T7 conditions. However rather large discrepancies are still observed, especially for the 7475 alloy. These differences might be related to the inhomogeneity in the distribution of intermetallic particles which was not taken into account in this model.

In the third model which was used, an attempt was made to take into account the influence of particle distribution. In a previous study [4] it was shown that J_{IC} and the critical cavity growth rate $(R/R_0)_c$ were related by the following expression :

$$J_{IC} = \beta \; M \; R_{p0.2} \cdot \Delta a_c . Ln \; (R/R_0)_c \quad (3)$$

It was found that β = 1.85 [1]. In Eq.3, Δa_c is assumed to be equal to the mean distance between particle clusters, λ_c in the fracture plane. This distance was determined metallographically : λ_c = 162 µm, 50 µm, 49 µm in the L-T, L-S, T-S planes for 7075 alloy and λ_c = 180 µm, 78 µm, 79 µm in the same planes for 7475 alloy. The values of $(R/R_0)_c$ were determined, as previously, from tests on notched specimens (Table 4). The results obtained from this model shown in Fig.4 give much better predictions for the fracture toughness of both alloys.

TABLE 4 - Critical cavity growth rate from tests on notched specimens

Alloy	7075			7475		
Direction	T351	T651	T7351	T351	T651	T7351
L	1.20	1.10	1.11	1.30	1.13	1.18
T	1.11	1.05	1.06	1.28	1.12	1.16
S	1.03	1.02	1.02	1.09	1.05	1.06

CONCLUSIONS

Tests on two Al alloys of the 7000 series have confirmed that the fracture toughness of these materials is largely dependent on the volume fraction of intermetallic particles, testing direction and heat-treatments. Three models based on the local approach to ductile fracture have been used to interpret the observed variations in fracture toughness. It is concluded that a model which takes into account the inhomogeneity in the distribution of inclusions leads to better predictions.

REFERENCES

(1) Achon, Ph., Ph. D. *Thesis Ecole des Mines*, Oct. 24, 1994.
(2) McMeeking, R.M.,*J. Mech. and Phys. of Solids*, Vol.25, 1977, pp.357-381.
(3) Lautridou,J.C.and Pineau,A., *Eng. Facture Mechanics*, Vol.15, 1981, pp.55-71.
(4) Mudry, F., Di Rienzo, F. and A. Pineau, *ASTM STP 995*, J.D. Landes et al Ed., 1989, pp.24-39.

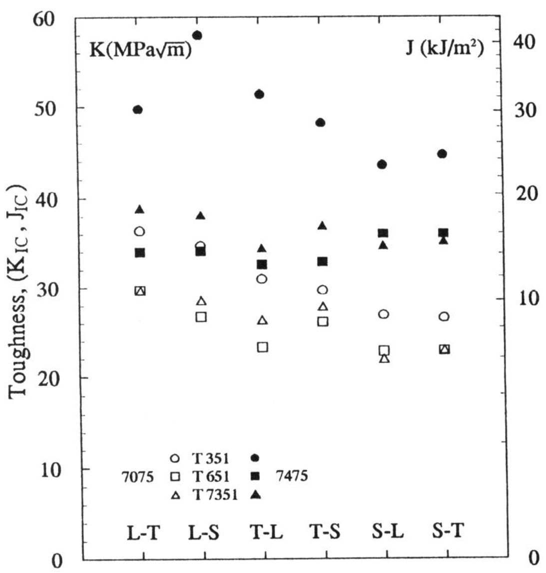

Figure 1 : Fracture toughness (K_{IC}, J_{IC}) of 7075 and 7475 alloys heat treated in three conditions and tested along six orientations.

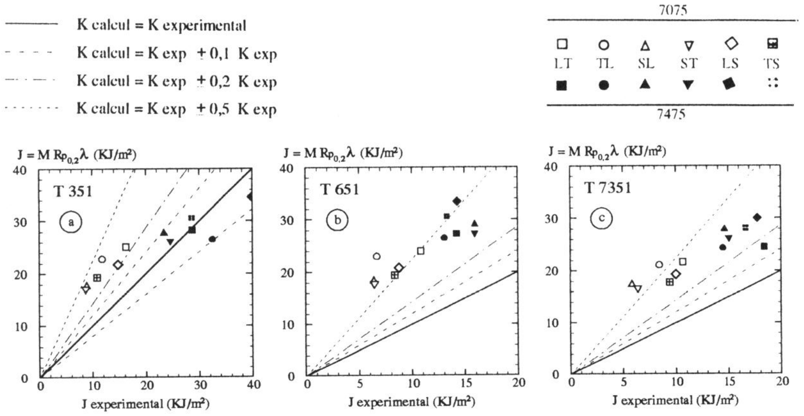

Figure 2 Model 1 : Comparaison of calculated and experimental J_{IC}.

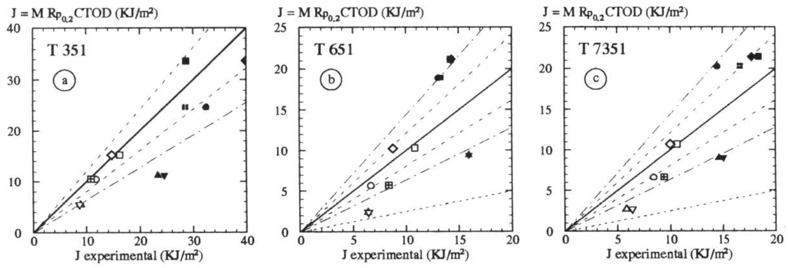

Figure 3 Model 2 : Calculated and experimental values of J_{IC}.

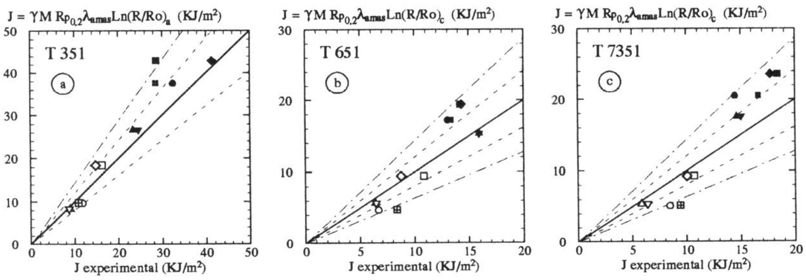

Figure 4 Model 3 : Calculated and experimental values of J_{IC}.